Validation of Hole-Drilling Residual Stress Measurements in Workpieces of Various Thickness

Lakey, Matthew Christopher
Hill, Michael R.

To be published in: Experimental Mechanics

DOI to publisher's version: 10.1007/s11340-024-01107-4

Experimental Mechanics (2024) 64:1529–1544
https://doi.org/10.1007/s11340-024-01107-4

RESEARCH PAPER

Validation of Hole-Drilling Residual Stress Measurements in Workpieces of Various Thickness

M. C. Lakey[1] · **M. R. Hill**[1]

Received: 25 March 2024 / Accepted: 16 August 2024 / Published online: 17 September 2024

Abstract

Background A recent revision to the ASTM E837 standard for near-surface residual stress measurement by the hole-drilling method describes a new thickness-dependent stress calculation procedure applicable to "thin" and "intermediate" workpieces for which strain versus depth response depends on workpiece thickness. This new calculation procedure differs from that of the prior standard, which applies only to thick workpieces with strain versus depth response independent of thickness.

Objective Herein we assess the new calculation procedures by performing hole-drilling residual stress measurements in samples with a range of thickness.

Methods Near-surface residual stress is measured in a thick aluminum plate containing near-surface residual stress from a uniform shot peening treatment, and in samples of different thickness removed from the plate at the peened surface. A finite element (FE) model is used to assess consistency between measured residual stress across the range of sample thickness.

Results Measured residual stress varies with sample thickness, with thinner samples exhibiting smaller near-surface compressive stress and a larger gradient of subsurface stress. These trends are consistent with both observed bending (curvature) of the removed samples and the trend in FE-calculated expected residual stress. The measured and expected residual stresses are in good agreement for samples of intermediate thickness, but the agreement decreases with sample thickness. Measured residual stress is invariant with gage circle diameter.

Conclusion The new thickness-dependent stress calculation procedure for hole-drilling provides meaningful improvement compared to thick-workpiece calculations.

Keywords Residual stress measurement · Hole-drilling method · Thin specimen · ASTM E837

Introduction

Hole-drilling is a widely used technique for measuring near-surface residual stress [1]. The essential elements of applying the technique are described in standard ASTM E837-20 [2]: a blind hole is drilled to a set of discrete depth steps through the center of a three-element strain gage rosette mounted to a flat workpiece; after drilling to each depth step, the in-plane strains measured by the three strain gages are recorded; after all depths have been drilled, the in-plane residual stresses at each depth step are calculated from the strain versus hole depth data. Prior work [1, 3] provides further guidance on key elements of the hole-drilling technique, including surface preparation, strain gage rosette selection, and drilling.

Research into the application of the hole-drilling method for residual stress measurement is both wide-ranging and ongoing. Previous work by Olson et al. [4] has discussed the precision and repeatability of residual stress measurements made by the hole-drilling method. Chighizola et al. [5] demonstrated the agreement of residual stresses measured using the hole drilling method with those measured by two other methods, slotting and x-ray diffraction. Studies by Madriaga et al. [6] and Chighizola et al. [7] made use of finite element methods alongside residual stress measurement by hole-drilling to predict deformation of parts due to machining-induced residual stresses. Further studies by Lord et al. [8] and Peng et al. [9] have investigated the use of digital image

M. R. Hill is a member of SEM.

✉ M. R. Hill
mrhill@ucdavis.edu

[1] Department of Mechanical and Aerospace Engineering, University of California, Davis, One Shields Avenue, Davis, CA 95616, USA

correlation as an alternative means of measuring relieved strain for hole-drilling residual stress calculation.

Much of the previous hole-drilling research has involved measurements in large, thick workpieces. However, the most recent revision to the hole-drilling standard (ASTM E837-20) adds methods for measuring residual stress in workpieces that are relatively thin, referred to as "thin" or "intermediate" thickness, relying on the recent work of Schajer [10]. The objective of this work is to perform residual stress measurements in workpieces of "thin" and "intermediate" thicknesses, using the new methods described in ASTM E837-20, and thereby assess their validity.

Methods

Materials and Geometry

This study uses a thick, aluminum alloy plate with one shot peened surface and samples removed from that plate. The plate geometry is cut from a large 25.4 mm thick AA 7050-T7451 rolled plate. The 7050 aluminum alloy is commonly used in aerospace structural applications and has been used in previous studies related to residual stress measurement [7, 11, 12]. The mechanical properties of this material in the T7451 temper are shown in Table 1 [13]. From the 25.4 mm thick plate, a smaller plate was machined to dimensions shown in Fig. 1, measuring 356 mm along the rolling direction (L) by 406 mm (long transverse, LT) by 20 mm (short transverse, ST). The 20 mm thickness was obtained by milling the original stock from only one 356 by 406 mm surface; the milled surface was designated as the top surface. Residual stress was induced in the plate by shot peening the top surface uniformly using SAE 170 cast steel shot at an Almen intensity of 6-10A and 100% coverage.

From the shot-peened plate, six smaller samples are cut as shown in Figs. 1 and 2, each measuring 102 mm (L) by 32 mm (LT) by 20 mm (ST). These samples are designated as samples A, B, C, D, E, and F and permanently inscribed with their letter designator in a corner of the shot-peened surface. Samples A through D are further cut to a specific, reduced thickness by wire electric discharge machining (EDM) on a plane parallel to the sample top (shot peened)

Table 1 Mechanical properties of AA7050-T7451 along the rolling (L) direction [13]

Material	Yield strength, S_y (MPa)	Ultimate strength, S_u (MPa)	Elastic modulus, E (GPa)	Poisson's ratio, ν	Elongation %
AA7050-T7451	459	524	71	0.33	10

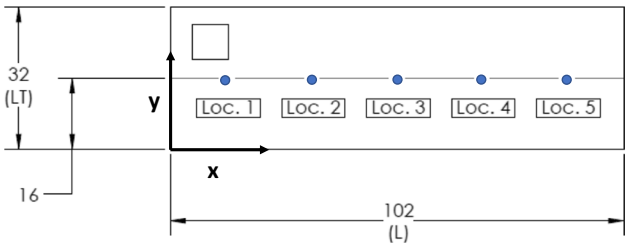

Fig. 2 Thin sample drawing showing hole-drilling measurement locations 1 to 5, top view; all dimensions in mm; box at upper left shows location of sample label (**A** to **F**)

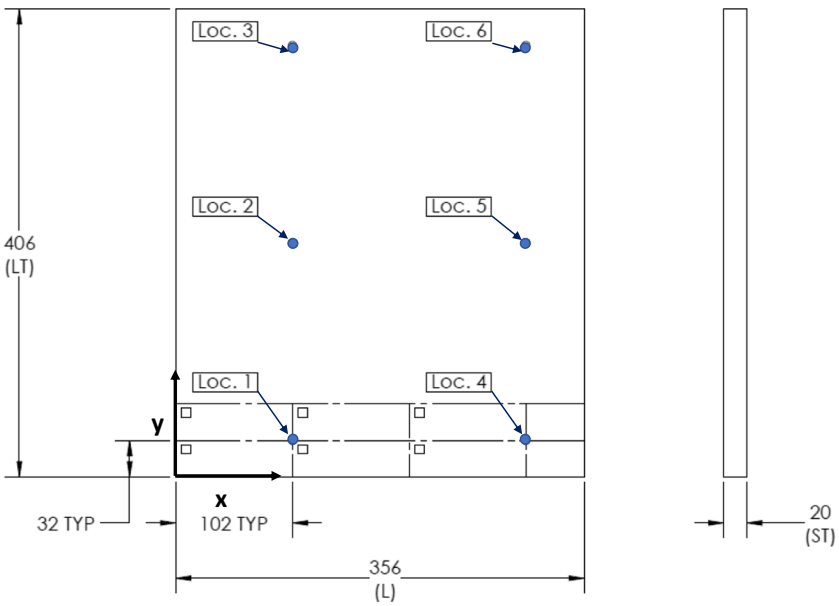

Fig. 1 Thick plate drawing showing hole drilling measurement locations 1 to 6, top and side views; cut locations for thin samples shown in dashed lines, with boxes showing location of sample labels (**A** to **F**); all dimensions in mm

Table 2 Workpiece thicknesses

Sample	Thickness, W (mm)	W/D (D = 5.13 mm)
A	1.25	0.244
B	1.5	0.292
C	2.0	0.390
D	3.0	0.585
Plate	20.0	3.90

surface, the plane being offset by the target workpiece thickness (see Table 2) plus half the wire EDM cut width. Samples E and F are set aside for further work. The four different final sample thicknesses fall into the range of "thin" or "intermediate" thickness for residual stress measurement by hole-drilling, as established by ASTM E837-20 [2] (and described further below).

Residual Stress Measurements

A series of residual stress measurements are performed in the shot peened plate and the removed samples using the hole-drilling method. Measurements follow ASTM E837-20 [2], which comprises the following steps. A strain gage rosette, having three individual strain gages positioned around a gage circle, is affixed to the workpiece surface. An end mill is used to mill a blind hole at the center of the gage circle in a series of prescribed depth steps. After reaching each depth step, strains measured by each of the three gages are recorded. Finally, after all depth steps are complete, the depth profiles of three in-plane components of residual stress are calculated from the strain versus hole depth data using the stress calculation procedure in ASTM E837-20 [2].

Each hole-drilling measurement incorporates the same materials and procedures, with key details as follows. Strain gage rosettes are Type A as defined in ASTM E837-20 [2] (Micro Measurements CEA-13-062UL-120), having a gage circle diameter of D = 5.13 mm. Rosettes are bonded to the workpiece using cyanoacrylate adhesive (Vishay M-Bond 200) and oriented such that Gage 1 of the rosette lays along the longitudinal (rolling) direction of the workpiece. The schedule of depth steps is shown in Table 3, which follows the procedure listed in ASTM E837-20, Sect. 8 [2] but adds smaller steps near the workpiece surface (depth < 0.3 mm). Holes are produced with a specialized milling station. Each measurement makes use of a new, 1.59 mm diameter, carbide end mill. The hole depth increments are cut such that the hole diameter is 2.0 mm using an orbital path with a spindle speed of 30,000 RPM, a plunge speed of 0.005 mm/s, and a travel speed of 1.0 mm/s. Measurements in the thick plate are performed with the plate clamped to the milling station table. Measurements in samples A, B, C, and D are performed with the samples clamped in a cantilevered configuration to a block on the milling station table. The cantilever clamping is used to avoid restraining deformation caused by hole-drilling, which is recommended for making useful measurements (see Schajer [1], Sect. 4.6). Figure 3 shows the cantilever clamping configuration; shims (not shown) are placed between the two clamps to avoid flattening existing sample curvature.

Table 3 Schedule of depth increments for hole-drilling for gage circle diameter D = 5.13 mm

Increment (mm)	Total depth (mm)
0	0
0.0254	0.0254
0.0254	0.0508
…	…
0.0254	0.3048
0.0508	0.3556
0.0508	0.4064
…	…
0.0508	1.016

Residual stress versus depth is calculated using the most recent revision to the hole-drilling standard, ASTM E837-20, and elastic properties in Table 1. Workpiece thickness ranges are designated in the standard using the ratio of workpiece thickness W to gage circle diameter D. Workpieces with W/D > 0.6 are designated as "thick"; this range of thickness is considered large enough that the strain versus depth response is independent of W. Workpieces with W/D < 0.25 are designated as "thin"; this range of thickness is considered small enough that the strain versus depth response is proportional to W. Workpieces with W/D between 0.25 and 0.6 are designated as "intermediate", where strain versus depth response depends on W in the manner described by Schajer [10]. Table 2 lists the thickness (W) and W/D values for the shot-peened plate and samples A, B, C, and D. The

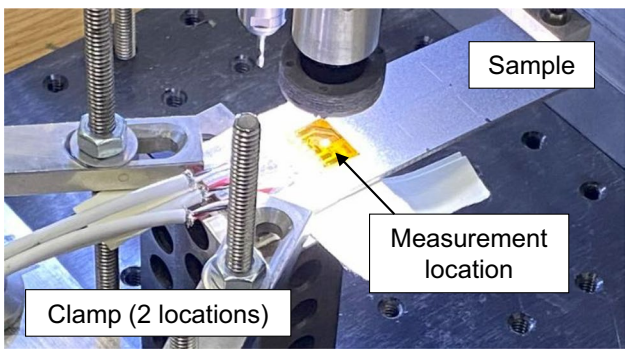

Fig. 3 Photo showing clamping configuration used for thin and intermediate samples

Table 4 Measurement locations for plate

Location	X-coordinate (mm)	Y-coordinate (mm)
1	102	32
2	102	203
3	102	375
4	305	32
5	305	203
6	305	375

Table 5 Measurement locations for removed samples

Location	X-coordinate (mm)	Y-coordinate (mm)
1	13	16
2	32	16
3	51	16
4	70	16
5	89	16

plate is a thick workpiece, sample A is a thin workpiece, and all other samples are intermediate workpieces.

A total of 17 residual stress measurements are performed: 5 measurements in the shot peened plate prior to cutting, and 3 measurements each on samples A, B, C, and D. Measurement locations for the plate are shown in Fig. 1 with coordinates listed in Table 4 (data reported for 5 of the 6 locations; one location was spare). Measurement locations on the smaller samples are shown in Fig. 2 with coordinates listed in Table 5 (data reported for 3 of the 5 locations; two locations were spare). The final hole depth is measured using a micrometer after each measurement is completed and the strain gage (and adhesive) removed. A depth offset is added to all depth steps so that the total of all depth steps matches the measured final depth [5].

Given the repeated hole-drilling measurements for each sample configuration, the average residual stress versus depth profile and its standard deviation are computed for further assessment. The residual stress versus depth data for each measurement is interpolated to mid-step depths of Table 3, the interpolation being necessary because the required depth corrections vary slightly among measurements. The average residual stress versus depth profile, and its standard deviation versus depth, is computed from the multiple measurements and reported. The data are also used for further assessment.

Data Assessment Using Elastic Stress Analysis

Although all samples are removed from a single plate that had been uniformly shot peened, the residual stress is expected to depend on the sample thickness. We expect that the uniformly shot-peened thick plate will have a thin layer of compressive stress at the peened surface that is balanced by low stresses away from the surface; therefore, the thick plate should not experience noticeable deformation after shot peening. However, we expect a thin sample removed from the surface of the same plate would deform, as the minimally stressed bulk of the plate is no longer present to resist the larger stresses near the peened surface. In deforming, a thin sample releases some of the near-surface compressive residual stress induced by the peening process; a thinner sample should have lower residual stress than a thicker sample, the thinner sample taking on a curvature indicative of the stress release. To quantify the deformation of each sample after removal from the plate by EDM cutting, we measure the EDM cut surface form using an area-scanning profilometer.

Because of the expected differences in residual stress among samples, a method is needed to compare residual stresses in the different thicknesses. One way to do this is to perform an elastic stress analysis [7] using a finite element (FE) model. Using a commercial FE code [14], a model is created for each sample thickness. Each model is rectangular with dimensions matching the sample, elastic material properties as given in Table 1, and the FE mesh composed of hexahedral elements. The mesh has 50 elements along each of the longitudinal (X) and long transverse (Y) directions. Element thickness in the short transverse (Z) direction is 0.0125 mm, resulting in 100 elements through thickness for sample A, 120 elements for sample B, 160 elements for sample C, and 240 elements for sample D.

For each sample thickness, the FE model takes an input stress versus depth profile and provides as an output relaxed residual stresses and a deformed sample shape. The input comprises an average residual stress versus depth profile for each in-plane stress component (longitudinal, transverse, and shear), developed by taking the average of the five measurements in the plate at each mid-step depth (where each depth step is defined in Table 3). The average stress versus depth profile of each stress component is input by setting a stress initial condition at the centroid of each element, using linear interpolation between depths as needed. For element centroids beyond the final mid-step depth in the plate, it is assumed that stress remains constant below the final mid-step depth; for centroids before the first mid-step depth, it is assumed that stress remains constant until the first mid-step depth. No other forces are imposed on the models. Constraints are applied only at the node at the center of the top surface: this node is fully constrained. Each model is allowed to reach equilibrium under these conditions. The output from each model is the longitudinal, transverse, and shear

residual stress through the thickness at the center of the sample. This output residual stress versus depth profile is called the expected residual stress profile. The expected residual stress profile from FE is compared to the measured residual stress profile by plotting them together, allowing a graphical comparison for each sample thickness. A quantitative comparison is performed by computing the root mean-square (RMS) difference between the expected and measured stress profiles.

Results

Thick Plate Residual Stress Measurements

Residual stress versus depth profiles measured in the thick plate are shown in Fig. 4. For all measurements, residual stress is negative (compressive) near the surface of the plate and increases in magnitude until reaching a minimum at a depth of roughly 0.1 mm; residual stress then decreases in magnitude until it approaches zero a depth of roughly 0.25 mm. A residual stress versus depth profile of this shape is typical for shot peened materials [15]. The maximum compressive stress in the longitudinal direction (σ_{xx}) is -300 ± 40 MPa; the maximum compressive stress in the transverse direction (σ_{yy}) is -315 ± 25 MPa. For all measurements in the thick plate, shear stress (σ_{xy}) was small (magnitude < 20 MPa) at all depth steps and is not therefore reported. The standard deviation of the measured residual stress in the thick plate is shown in Fig. 5. The standard deviation of the measurements is maximum (45 MPa for longitudinal stress and 60 MPa for transverse stress) at the first depth increment (0.0127 mm); decreases rapidly until a depth of roughly 0.1 mm; increases again to a local maximum at 0.14 mm (30 MPa for both longitudinal and transverse stress); and finally decreases rapidly to values of 10 MPa or less in the subsurface region (depths past 0.3 mm).

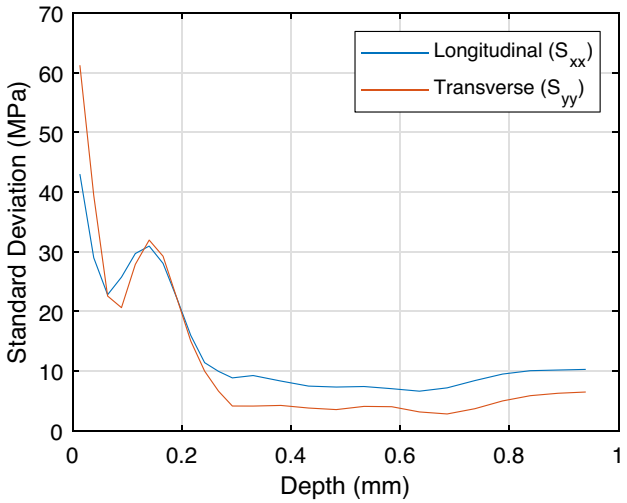

Fig. 5 Standard deviation of residual stress versus depth for five replicate measurements in 20 mm thick plate

Thin and Intermediate Sample Residual Stress Measurements

Figure 6(a) shows a comparison of longitudinal strain versus hole depth for one representative measurement in the thick plate and each removed sample (data in Fig. 6(b) are described later). For shallow depths (depth < 0.2 mm), the strain versus hole depth behavior is similar for all removed samples, rising to roughly 100 με at a depth of roughly 0.18 mm, with those strains being lower than strains in the thick plate. Past this depth, the strain versus hole depth behavior varies significantly with workpiece thickness. For samples A, B, and C, the strain begins to fall at hole depths past 0.2 mm, with the thinner samples approaching zero strain more rapidly than in the thicker samples. For sample D, the strain continues to increase slowly until reaching a maximum (of roughly 125 με) at a hole depth of 0.4 mm, then slowly decreasing with greater depth. The strain versus hole depth behavior in the thick plate differs completely

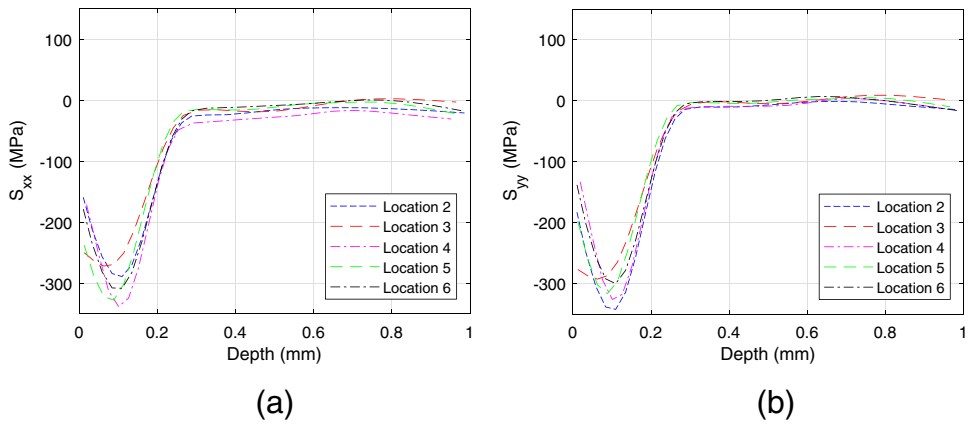

Fig. 4 Residual stress from five replicate measurements in thick plate (20 mm thick): (**a**) longitudinal and (**b**) transverse

from that in the removed samples, with the strain being larger and then continuing to increase for all depths.

Figure 7 shows residual stress for sample D; Fig. 8 for sample C; Fig. 9 for sample B; and Fig. 10 for sample A. A comparison of average residual stress versus depth profiles for all samples, as well as the thick plate, can be found in Fig. 11(a) and (b). For all measurements, the normal components of residual stress are negative (compressive) near the surface of the sample and increase in magnitude until reaching a minimum at a depth of roughly 0.09 mm; residual stress then increases until reaching a maximum at a depth of roughly 0.25 mm, and finally decreases slowly over greater depths. The average maximum compressive stress in the longitudinal direction (σ_{xx}) is -218 MPa for sample D, -205 MPa for sample C, -171 MPa for sample B, and -141 MPa for sample A. The average maximum compressive stress in the transverse direction

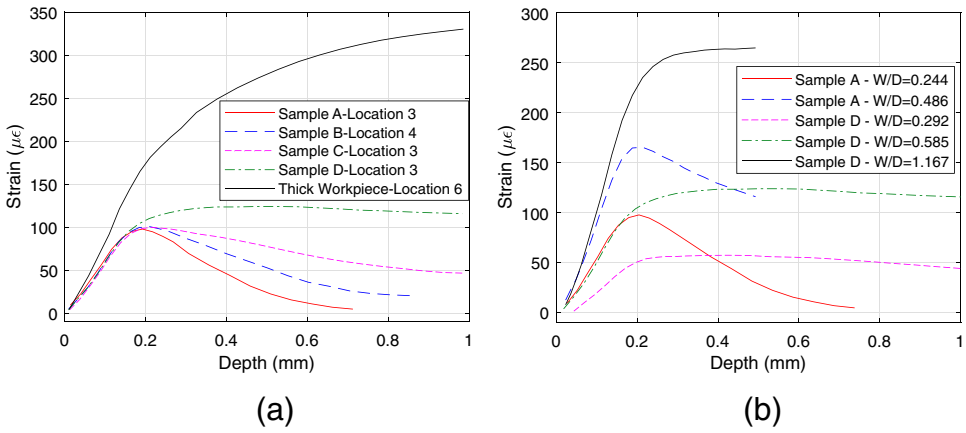

Fig. 6 Longitudinal strain versus hole depth for: (**a**) representative measurements in all sample thicknesses and (**b**) measurements with various gage circle diameter D in sample A (1.25 mm thick) and sample D (3.0 mm thick)

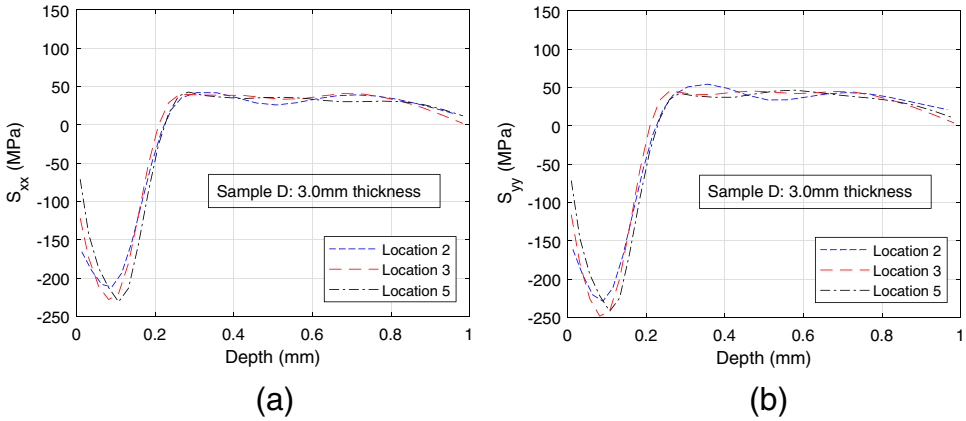

Fig. 7 Residual stress from three replicate measurements in sample D (3.0 mm thick): (**a**) longitudinal and (**b**) transverse

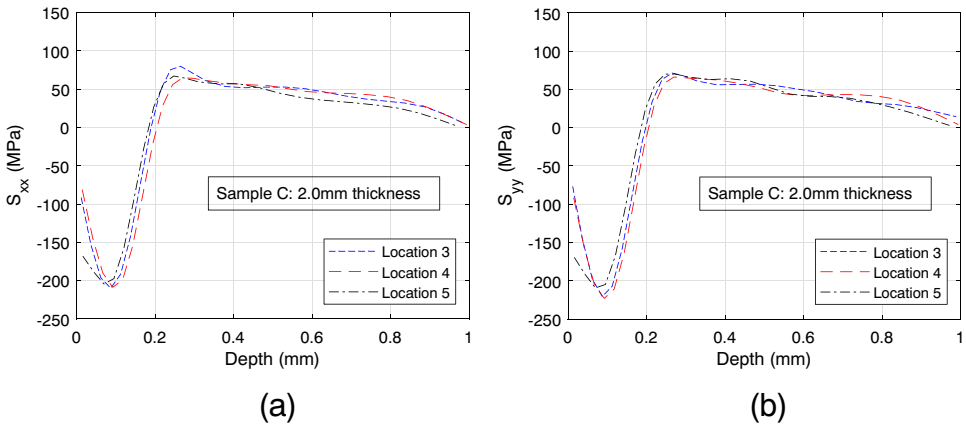

Fig. 8 Residual stress from three replicate measurements in sample C (2.0 mm thick): (**a**) longitudinal and (**b**) transverse

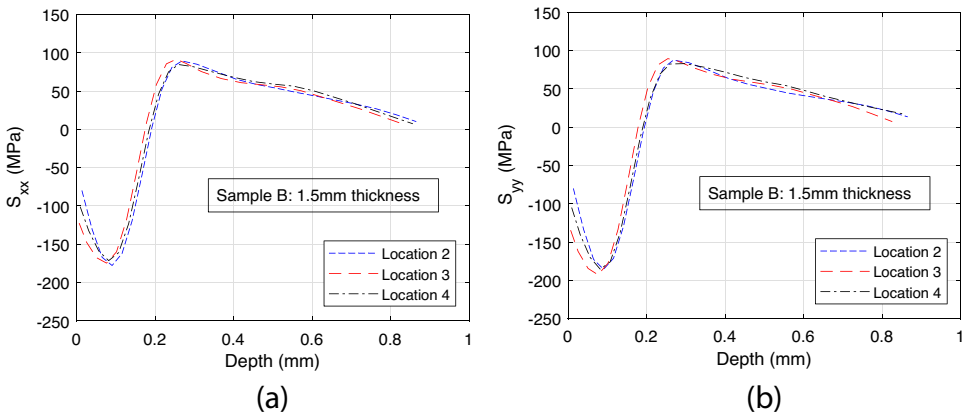

Fig. 9 Residual stress from three replicate measurements in sample B (1.5 mm thick): (**a**) longitudinal and (**b**) transverse

(σ_{yy}) is consistently larger in magnitude than in the longitudinal, being -234 MPa for sample D, -215 MPa for sample C, -184 MPa for sample B, and -157 MPa for sample A. For all samples, shear stress (σ_{xy}) was small (magnitude < 20 MPa) for all depth increments and is not therefore reported. The residual stress in the removed samples (Fig. 11) matches typical behavior for shot peened material, but the magnitude of the compressive stress increases with thickness, and the slope of the subsurface stress (beyond 0.3 mm) decreases with thickness. This matches our expectation that thin samples experience a stress release when removed from the thicker plate, with thinner samples experiencing a larger stress release.

The standard deviation of the replicate measurements in each sample are shown in Fig. 12 and included as error bars in Fig. 11. For all samples and for both longitudinal (σ_{xx}) and transverse (σ_{yy}) directions, the standard deviation is maximum at the initial depth step; reaches a local minimum at a depth of roughly 0.09 mm (approximately the depth at which the residual stress profile reaches its minimum value); reaches another local maximum at a depth of roughly 0.15 mm; and finally decreases to relatively small (0–10 MPa) values by a depth of roughly 0.03 mm and remains relatively small for the rest of the depth steps. For samples A and B, the maximum standard deviation is 30.0 ± 5.0 MPa for both longitudinal and transverse stresses; for sample C, the maximum standard deviation is 47.5 ± 1.0 MPa for both longitudinal and transverse stresses; for sample D, the maximum standard deviation is 40.0 ± 2.0 MPa for both longitudinal and transverse stresses. It is notable that thinner samples did not exhibit larger standard deviation (more dispersion) as compared to thicker samples.

Data Assessment Using Elastic Stress Analysis

Figure 13 shows the form of the EDM surface of each sample after cutting from the thick plate by wire EDM. A radius of curvature is computed from each surface form by using circular fits to surface height data along two lines, one along the X-direction and the other along the Y-direction, both lines being near the middle of the samples. Table 6 compares radii of curvature for the samples. The radius of curvature is smallest for the thinnest sample (A) and largest for the thickest sample (D). This suggests that thinner samples experienced a greater release of stress during EDM cutting, which is consistent with the residual stress of Fig. 11.

Expected residual stress (based on FE modelling) is shown for all sample thicknesses in Fig. 11(c) and (d). The trends in expected residual stress with thickness generally agree with those for the measured residual stress (Fig. 11(a) and (b)). The magnitude of the peak compressive stress

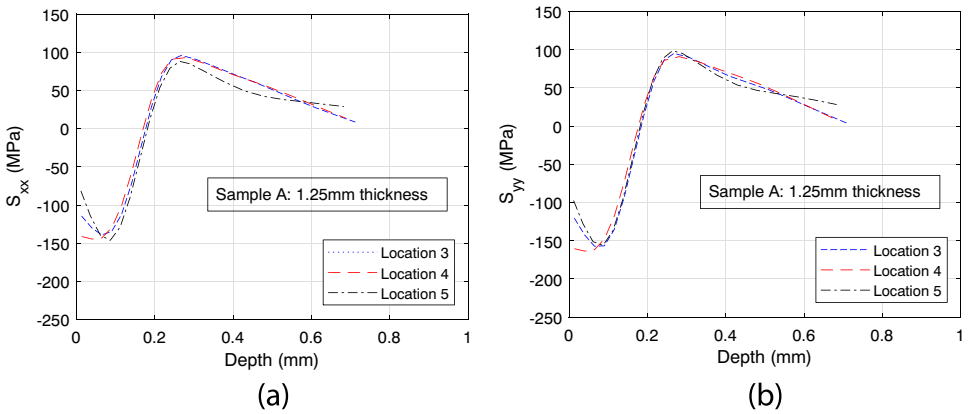

Fig. 10 Residual stress from three replicate measurements in sample A (1.25 mm thick): (**a**) longitudinal and (**b**) transverse

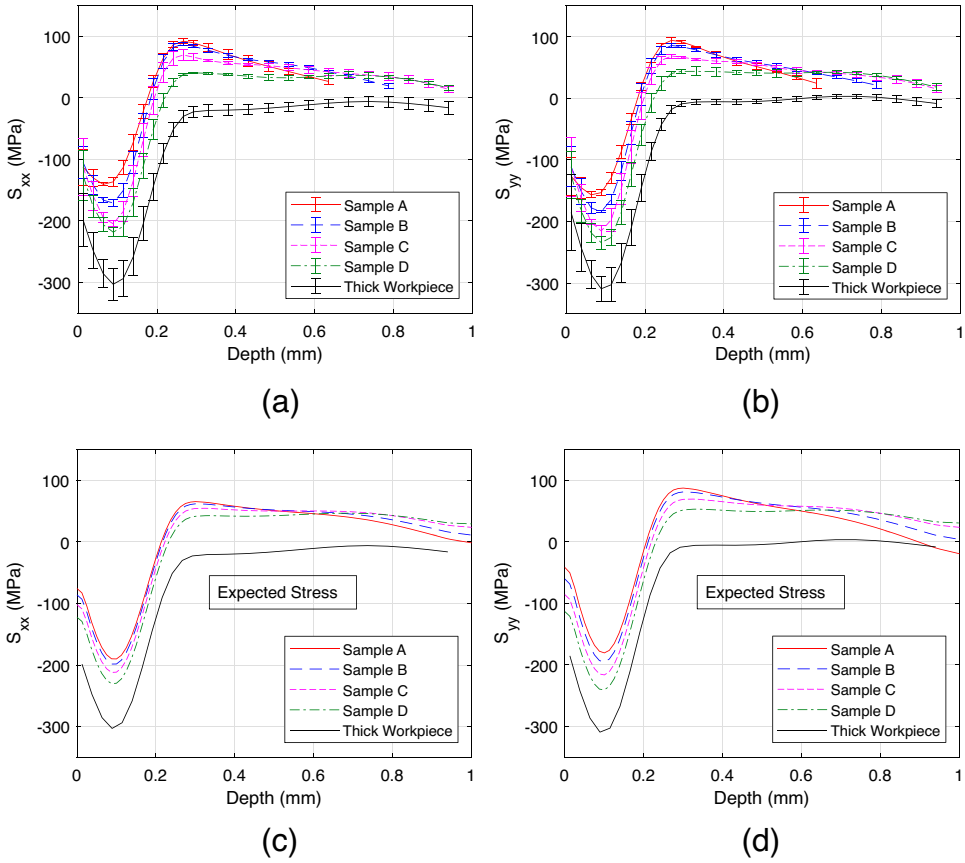

Fig. 11 Residual stress for all sample thicknesses: average measured (**a**) longitudinal and (**b**) transverse, and expected (based on FE), (**c**) longitudinal and (**d**) transverse; error bars in (**a**) and (**b**) reflect standard deviation of replicate measurements

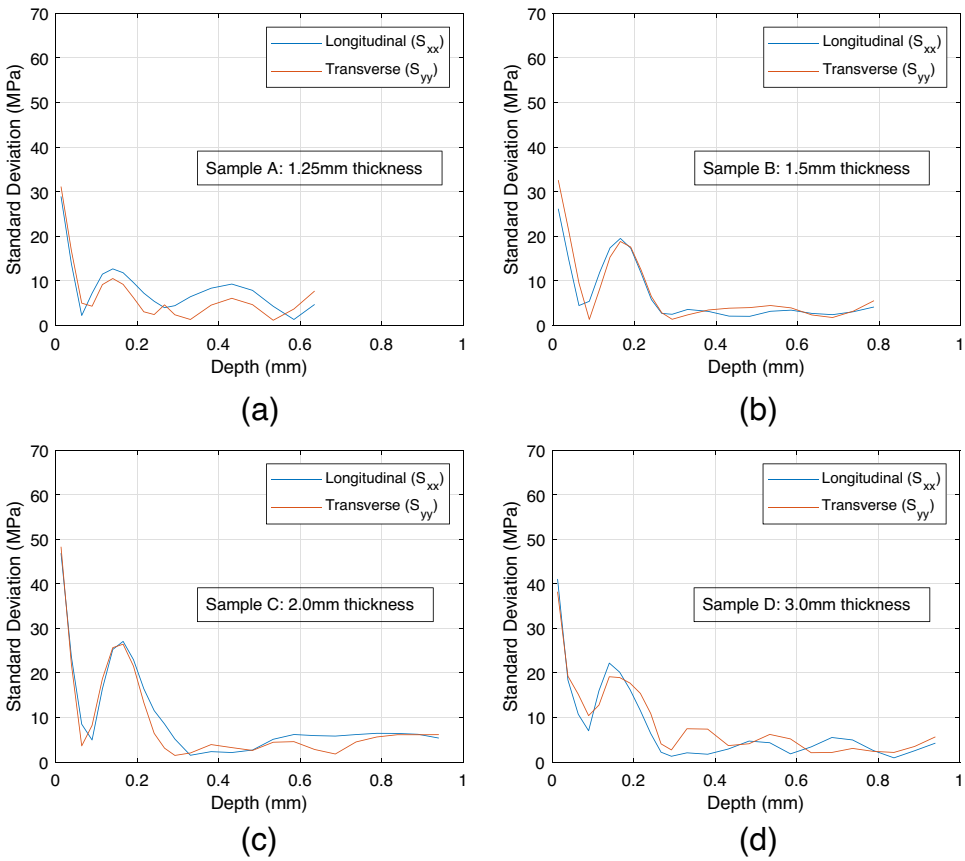

Fig. 12 Standard deviation of residual stress versus depth for all measurements: (**a**) sample A (1.25 mm thickness), (**b**) sample B (1.5 mm thickness), (**c**) sample C (2.0 mm thickness), (**d**) sample D (3.0 mm thickness)

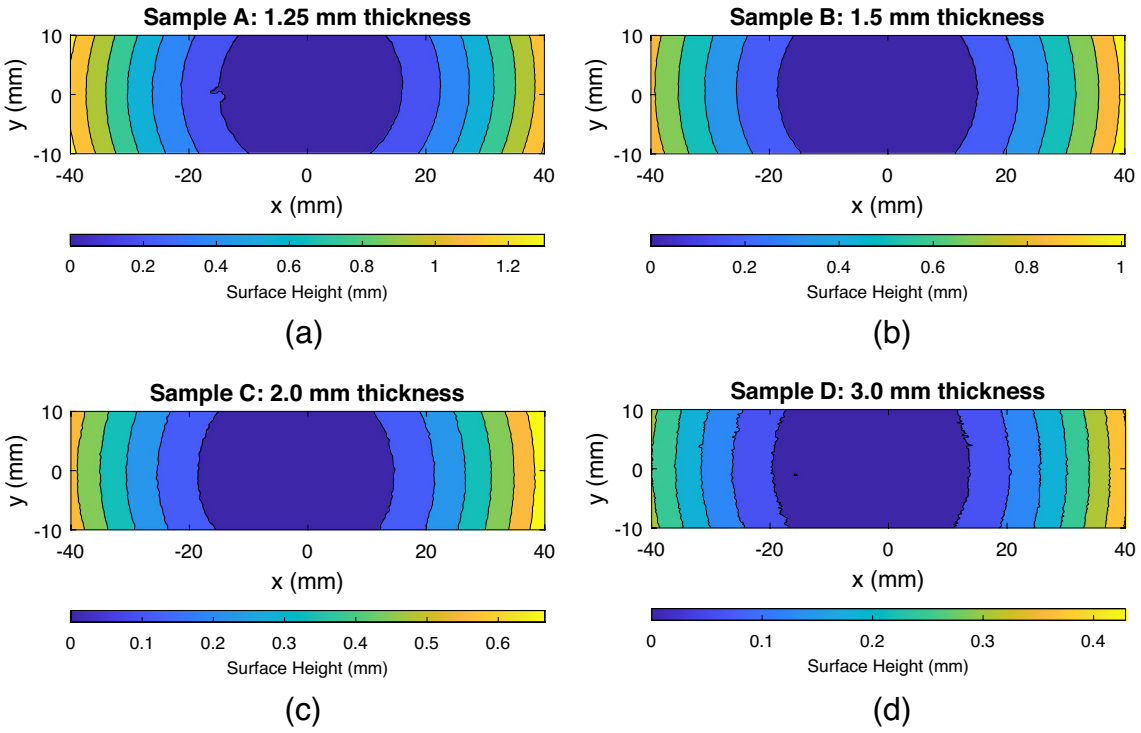

Fig. 13 Contour plots of the EDM surface form for each sample: (**a**) sample A (1.25 mm thickness), (**b**) sample B (1.5 mm thickness), (**c**) sample C (2.0 mm thickness), (**d**) sample D (3.0 mm thickness)

Table 6 Measured sample thickness and radii of curvature

Sample	Measured thickness (mm)	Radius of curvature, longitudinal (mm)	Radius of curvature, long transverse (mm)
A	1.26	643	585
B	1.53	834	834
C	2.03	1220	1340
D	3.03	2210	2630

Table 7 RMS difference between average residual stress and expected residual stress profiles

Sample	σ_{xx} (MPa)	σ_{yy} (MPa)
A	43.26	35.45
B	31.95	25.21
C	23.09	20.23
D	12.56	11.21

increases with sample thickness while the subsurface (depth > 0.3 mm) slope decreases with sample thickness.

While Fig. 11 shows general agreement between measured and expected residual stress, the measured stresses are more significantly affected by thickness than are the expected stresses, especially for small thickness. For the smallest thickness (sample A), the measured longitudinal peak compression is -140 MPa while the expected peak is -190 MPa, which is a significant difference. For the intermediate thickness (sample D), the measured and expected longitudinal peak compression are similar (about -220 MPa). The measurement data also suggest that thickness affects the depth at which the peak compression occurs, being shallower in the smallest thickness (sample A). The subsurface (depth > 0.3 mm) stress gradient is similarly affected, the measured and expected longitudinal stress gradient being in reasonable agreement for the intermediate thickness (sample D) and quite different for the smallest thickness (sample A). The RMS differences between the average measured residual stress profile and the expected residual stress profile are given in Table 7 for longitudinal and transverse stress in each sample. The table shows that RMS difference is largest for the smallest thickness and decreases steadily with increasing thickness; the RMS difference is mostly independent of the stress direction.

Discussion

Comparison of Thick Plate Residual Stress to Previous Work

It is useful to compare the thick plate residual stress versus depth data (Fig. 4) to prior work. Numerous previous studies

[4, 11, 16–18] provide residual stress measurement data for AA 7050-T7451 workpieces treated with similar (although not identical) shot peening parameters, with residual stress measurements by hole-drilling, slitting, and x-ray diffraction with layer removal. Figure 14 compares the average longitudinal residual stress versus depth profile in the present thick plate to data from the prior studies. The data show similar trends, with surface stress of -100 to -150 MPa giving way to maximum compressive stress of -250 to -300 MPa at a depth of 0.07 to 0.10 mm, and a depth of compression (zero crossing) of about 0.30 mm. Overall, we conclude that the present thick plate residual stresses are typical of shot peened aluminum plate.

Comparison of Thick and Thickness-Dependent Calculation Procedures

To quantify the value of the new residual stress calculation procedure for intermediate and thin workpieces in ASTM E837-20, we perform additional residual stress calculations for one measurement in each sample using the thick workpiece calculation procedure. It is expected that the thick workpiece calculation procedure, when inappropriately used for intermediate and thin samples, will produce erroneous residual stress results relative to those from the thickness-dependent calculation procedure. Figures 15 and 16 compare the two normal residual stress components calculated using the two procedures. For sample D, with W/D (0.585) just below the threshold for a thick workpiece (W/D = 0.6), the two procedures give similar results. For smaller W/D, the thick workpiece procedure exaggerates the minimum and maximum stress values, the exaggeration being larger for smaller thickness. For the smallest thickness (sample A with W/D = 0.244), the thick workpiece calculation exaggerates the minimum stress by 60 to 90 MPa and the maximum stress by 60 MPa. Figures 15 and 16 also show that stresses from the thick workpiece procedure have roughly the same maximum compressive stress for every sample thickness; constant maximum compressive stress with decreasing thickness is erroneous and arises from not using the thickness-dependent calculation procedure. We conclude that the thickness-dependent residual stress calculation procedure provides value, as it produces the expected trends in residual stress for thin and intermediate samples that the thick workpiece calculation fails to capture.

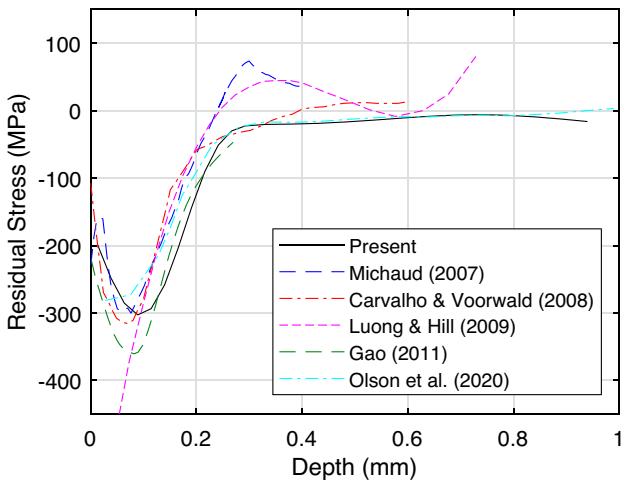

Fig. 14 Present thick plate residual stress versus depth profile compared to similar prior work

Measurements on Reverse Surface of Samples

To provide an additional comparison for the FE-calculated expected residual stress, two additional hole-drilling measurements are performed on the back (EDM) surface (opposite the shot-peened top surface) of two samples, one on sample A (1.25 mm thickness), and one on sample D (3.0 mm thickness). Figure 17 displays measured residual stress data for sample A, with the average of measurements on the top surface and the single measurement on the back surface, along with the expected residual stress for sample A. Figure 18 displays a similar comparison for sample D. Inspection of Figs. 17 and 18 shows that, for both samples A and D, the residual stress measured near the back surface falls close to the expected stress (notwithstanding a sharp increase in measured residual stress within roughly 0.1 mm of the back surface that is consistent with localized tensile stresses created by wire EDM). The similarity is encouraging.

Bending Stress from Curvature

Figures 17 and 18 include an estimate of the bending stress in the two samples, which is computed from the measured radii of curvature (Table 6) using a strength of materials (SoM) analysis. SoM relates the radius of curvature in beam bending to a linear distribution of stress through the beam thickness. The dashed lines in Figs. 17 and 18 reflect this trend, computed by combining the moment–curvature relation with the typical equation for bending stress, which provides

$$\sigma = \frac{Ey'}{\rho} \tag{1}$$

where E is the elastic modulus (Table 1), ρ is radius of curvature (Table 6), and y' is distance from the beam mid-thickness. For both samples the slope of the bending stress from SoM is in excellent agreement with the slope of hole-drilling

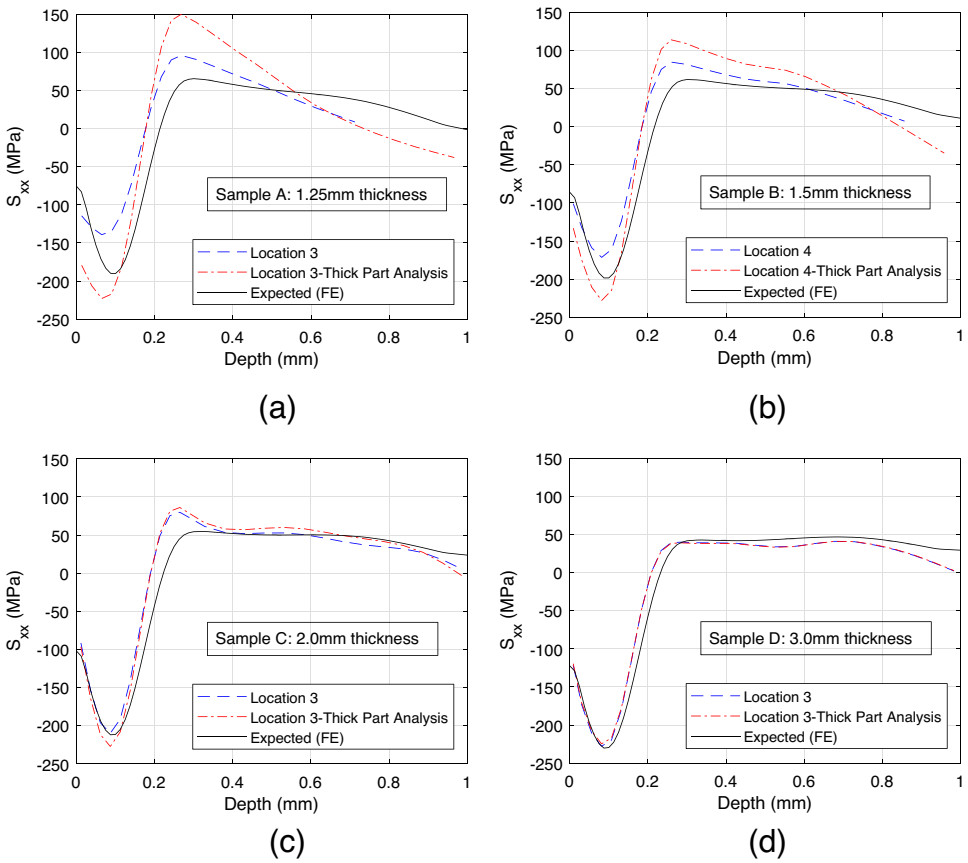

Fig. 15 Longitudinal residual stress versus depth for representative measurements: (**a**) sample A (1.25 mm thickness), (**b**) sample B (1.5 mm thickness), (**c**) sample C (2.0 mm thickness), (**d**) sample D (3.0 mm thickness); plots show profiles calculated using the new thickness-dependent procedure, the prior thick-workpiece procedure, and expected from FE

data at the back surface and the expected stress (from FE); this trend holds for both longitudinal and transverse stresses. Figure 17 shows that the slope of the front surface measurement data, at depths from 0.3 to 0.6 mm, does not match the slopes of the other trends (SoM bending stress, expected stress, or the back surface stress). A similar outlying trend of front surface measured stress is not evident for sample D in Fig. 18. We conclude that there may be some systematic error in the measurement technique used for sample A or perhaps in the thin-workpiece residual stress calculation procedure.

Effect of Clamping

The goals of clamping for hole-drilling residual stress measurements are: first, to secure the sample to achieve good precision in cutting; second, to introduce near-zero strain (not flatten existing sample curvature); and third, to allow the sample to deform after cutting each hole depth step. These goals are easily met for the thick plate by applying clamps at locations relatively far (greater than 100 mm) from the site of the strain gage rosette. However, proper clamping of the thin and intermediate thickness samples is more difficult, as their non-flat geometry (Fig. 13) causes conflict between the goals listed above. The cantilever configuration (Fig. 3) has clamps applied within 25 mm of the strain gages, due to the small sample size, and shims are used to reduce clamping strain. This allows clamping with a strain of no more than 7 με.

To evaluate the effect of clamping on hole-drilling measurements in sample A, two additional measurements are performed with the sample firmly clamped, as shown in Fig. 19. Measurements are located either at the main sites shown in Fig. 2 or mid-way between those sites. Figure 20 compares residual stress versus depth data for measurements with the normal cantilever clamping (normal, Fig. 3) and with firm clamping. For shallow depth (< 0.2 mm), the firmly-clamped data agree closely with the expected stress, including the magnitude and depth of maximum compressive stress. At larger depths (0.2 to 0.4 mm) the two measurements diverge from one another.

For purposes of comparison, it is useful to add the residual stresses from the sample in the normal cantilever clamping configuration to the additional stress introduced to the sample by firm clamping. This "corrected" residual stress (from the normal clamping measurements) can be compared to the residual stress from the firmly-clamped measurements to determine whether the agreement of the firmly-clamped measurements with the expected residual stress is solely due

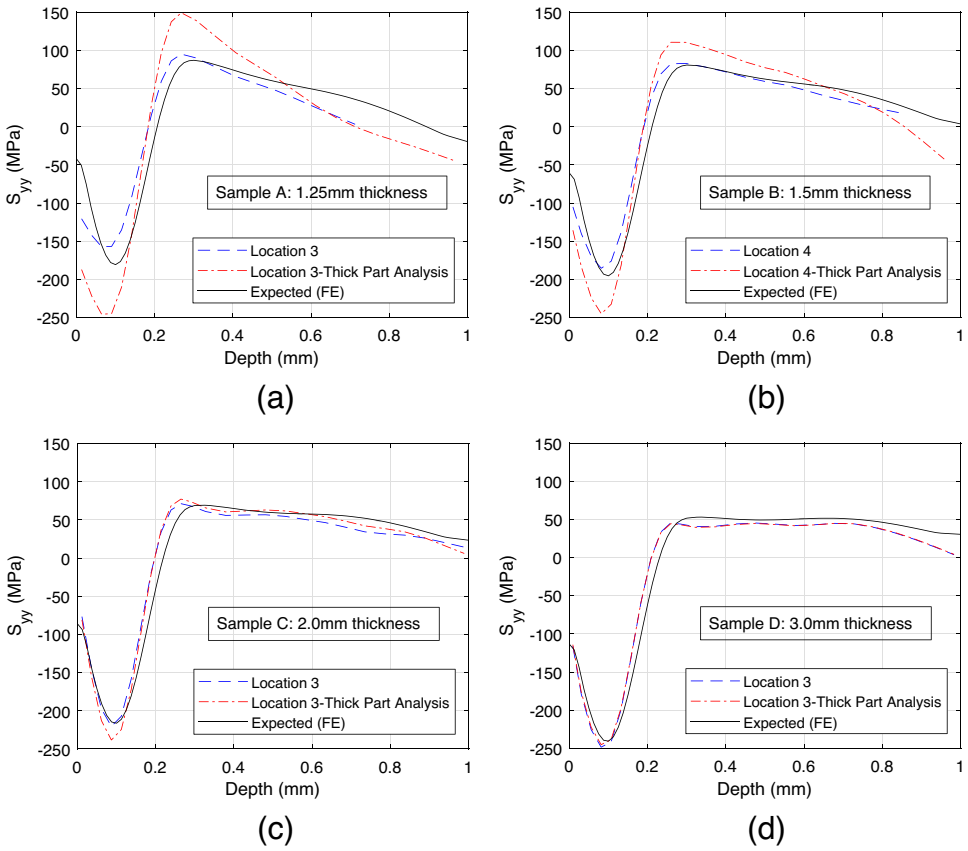

Fig. 16 Transverse residual stress versus depth for representative measurements: (**a**) sample A (1.25 mm thickness), (**b**) sample B (1.5 mm thickness), (**c**) sample C (2.0 mm thickness), (**d**) sample D (3.0 mm thickness); plots show profiles calculated using the new thickness-dependent procedure, the prior thick-workpiece procedure, and expected from FE

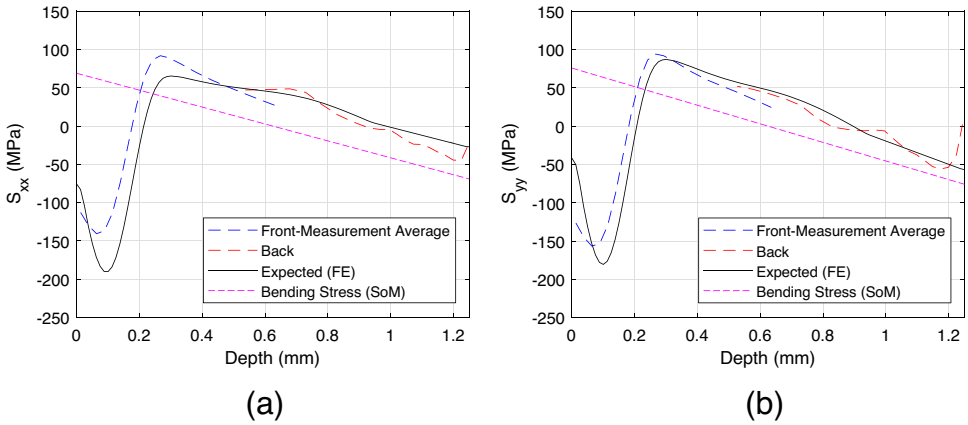

Fig. 17 Residual stress from average of three measurements in front surface and one measurement in reverse surface of sample A (1.25 mm thick): (**a**) longitudinal and (**b**) transverse; expected (based on FE) and bending (based on SoM) residual stress also included

to the addition of clamping stress. The clamping stresses are estimated as bending stresses, with the surface stress computed from strains measured after clamping. Clamping strains in the second firm-clamping measurement are as follows: -966 με in gage 1 (along the longitudinal direction), -578 με in gage 2 (45°), and -232 με in gage 3 (90°). Surface stresses calculated from these strains using planar stress–strain relations give σ_{xx} of -83 MPa and σ_{yy} of -44 MPa. The corrected normal cantilever clamping data (Fig. 21) show similar maximum compressive stress to the firmly-clamped data, and the two datasets behave similarly past the depth of maximum compressive stress. However, the firmly-clamped data agree more closely with the expected stress than the corrected normal cantilever clamping data at shallow depths. This suggests that the difference between the residual stress profiles measured with normal cantilever clamping and firm clamping is not solely due to the introduction of clamping strains. While there is improved agreement between the firmly-clamped measurements and the expected stress, the firm clamping conflicts with good

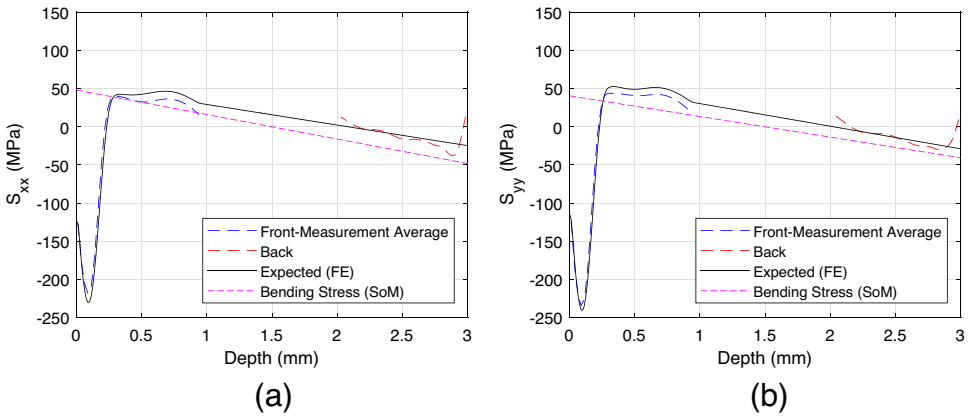

Fig. 18 Residual stress from average of three measurements in front surface and one measurement in reverse surface of sample D (3.0 mm thick): (**a**) longitudinal and (**b**) transverse; expected (based on FE) and bending (based on SoM) residual stress also included

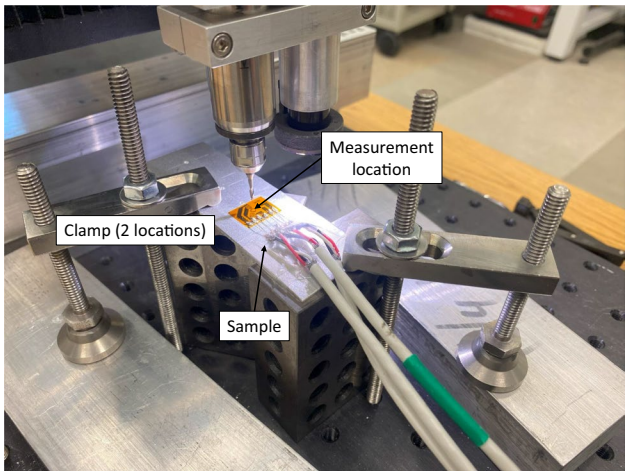

Fig. 19 Photo showing clamping configuration used for firm-clamping measurements in sample A (1.25 mm thickness)

practices described by Schajer [1] and NPL [3]. It would be useful to assess the effects of clamping for thin samples in further work.

Comparison of Residual Stress Measurements Using Various Gage Circle Diameters

To further probe the relationship between sample thickness and measured residual stress, an additional set of hole-drilling experiments is performed. The main set of experiments address the influence of W/D by varying W (thickness) while keeping D (gage circle diameter) constant at 5.13 mm. The set of additional measurements varies the gage circle diameter, with measurements in two samples. In sample A (1.25 mm thickness), one additional measurement is performed using a strain gage rosette with a gage circle diameter of 2.57 mm. In sample D (3.0 mm thickness), two additional measurements are performed, one each with gage circle diameters of 2.57 mm and 10.26 mm. These complement the prior measurements with a gage circle diameter of 5.13 mm. The schedule of depth steps used for the additional measurements are in Table 8 (2.57 mm diameter) and Table 9 (10.26 mm). The hole diameter is 1 mm and 4 mm for the small and large size gages respectively. Varying the gage circle diameter on a single sample thickness changes the value of W/D and therefore changes the residual stress calculation procedure and, possibly,

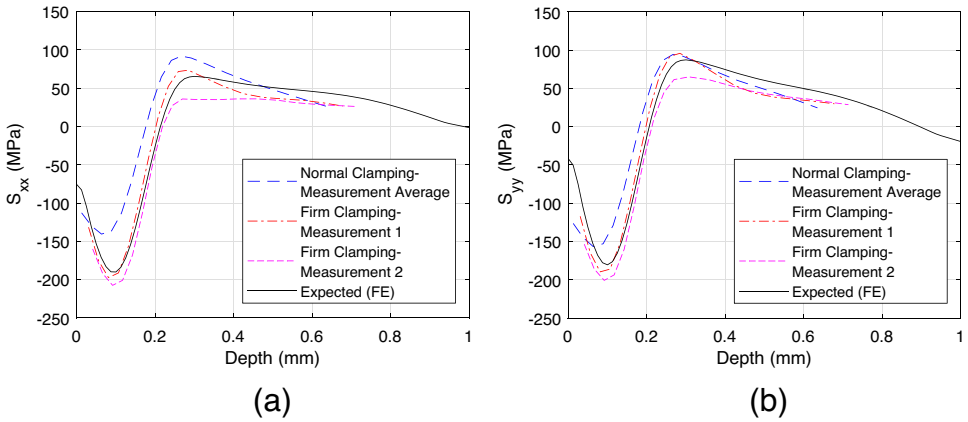

Fig. 20 Residual stress from average of three measurements with normal clamping and two measurements with firm clamping, in sample A (1.25 mm thick): (**a**) longitudinal and (**b**) transverse; expected (based on FE) residual stress also included

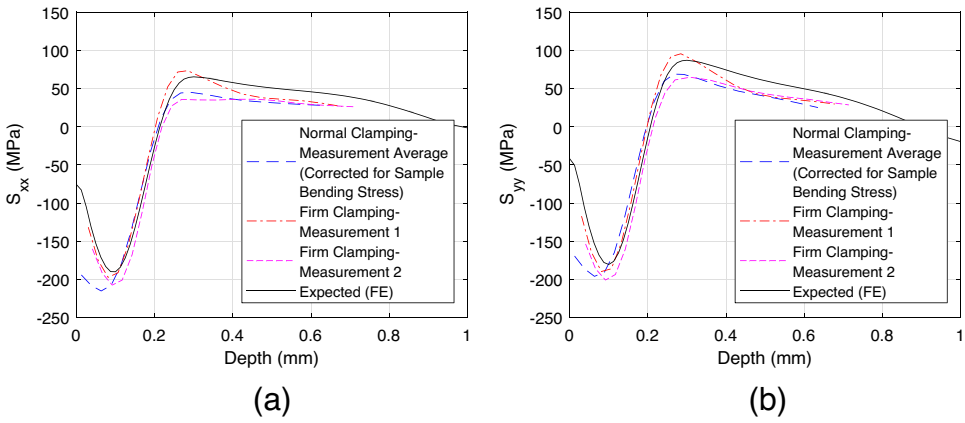

Fig. 21 Residual stress from average of three measurements with normal clamping (corrected for sample bending stress) and two measurements with firm clamping, in sample A (1.25 mm thick): (**a**) longitudinal and (**b**) transverse; expected (based on FE) residual stress also included

Table 8 Schedule of depth increments for hole-drilling for gage circle diameter D = 2.57 mm

Increment (mm)	Total depth (mm)
0	0
0.0127	0.0127
0.0127	0.0254
…	…
0.0127	0.1270
0.0254	0.1524
0.0254	0.1778
…	…
0.0254	0.5588

Table 9 Schedule of depth increments for hole-drilling for gage circle diameter D = 10.26 mm

Increment (mm)	Total depth (mm)
0	0
0.0254	0.0254
0.0254	0.0508
…	…
0.0254	0.3048
0.0508	0.3556
0.0508	0.4064
…	…
0.0508	1.0668

the sample thickness designation. For example, the original measurement on sample A has W/D = 0.244, which is designated as "thin"; however, the follow-on measurement with gage circle diameter 2.57 mm has W/D = 0.486, which is designated as "intermediate".

Data from the additional set of measurements underscore how W/D affects strain release and the residual stress calculation. Figure 6(b) compares longitudinal strain versus hole depth for measurements on sample D with gage circle diameters D = 2.57 mm (W/D = 1.17), D = 5.13 mm (W/D = 0.585), and D = 10.26 mm (W/D = 0.292). The strains depend strongly on gage circle diameter, with smaller gages (larger W/D) experiencing larger strains. Figure 22 compares residual stress data for measurements in sample A (for two values of W/D) while Fig. 23 compares the data for sample D (for three values of W/D). For both samples (A and D), the residual stress data are comparable at all depths regardless of gage circle diameter, despite the obvious differences in measured strain (Fig. 6(b)). Some differences are observed in measured residual stress values using various gage circle diameters at the first depth step (0.0127 mm or 0.0254 mm, depending on the gage circle diameter used). However, we note that even for measurements using the same sample and gage circle diameter, the standard deviation of the measured residual stress is largest at the first depth step, as shown by the error bars in Figs. 22 and 23. Shortly after the first depth step (at a depth of approximately 0.05 mm), the trend of measured residual stress data for all gage circle diameters begin to match more closely, and the trend remains similar through the full depth of the measurement. This suggests that the new thickness-dependent residual stress calculation procedure produces results that are independent of gage circle diameter, thereby validating the new thickness-dependent residual stress calculation procedure.

Conclusion

The objective of this work is to perform residual stress measurements in thick, thin, and intermediate workpieces to validate the new thickness-dependent stress calculation procedure in ASTM E837-20. Hole-drilling residual stress measurements are performed in a thick shot peened plate, and in several samples removed from the plate and having various thicknesses. Furthermore, residual stress measurements in the thick plate are used as the basis for FE modelling of the expected residual stress in the removed thin

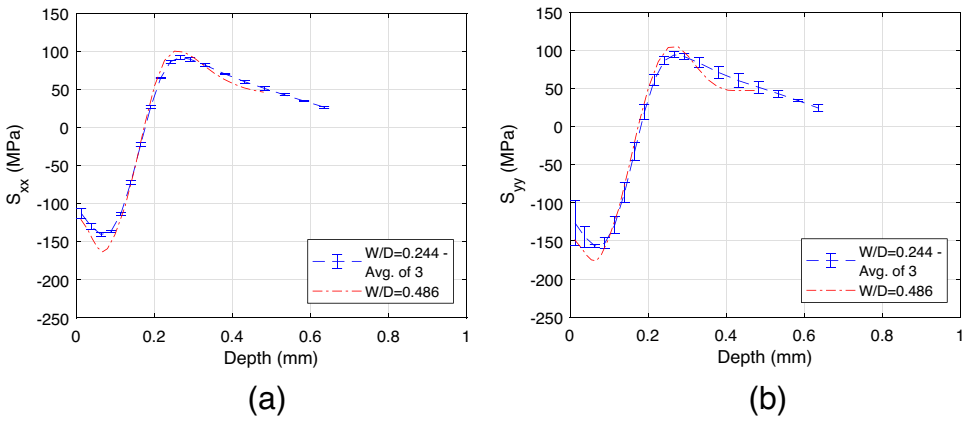

Fig. 22 Residual stress from average of three measurements with W/D = 0.244 and one measurement with gage size W/D = 0.486, in sample A (1.25 mm thick): (**a**) longitudinal and (**b**) transverse

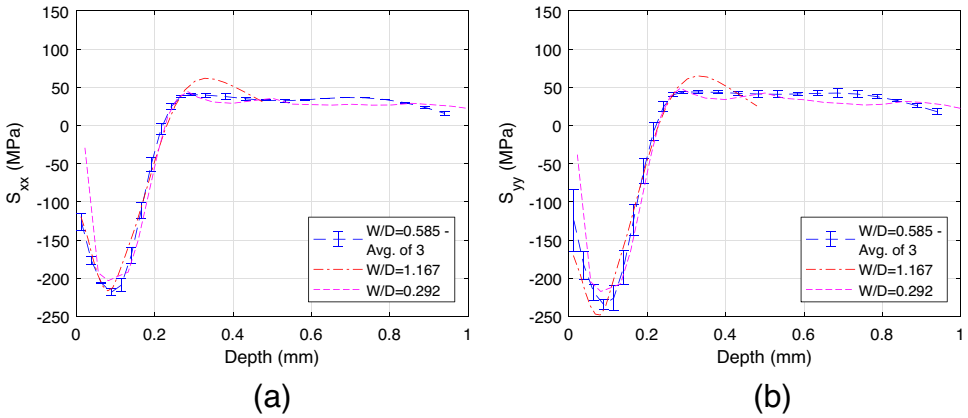

Fig. 23 Residual stress from average of three measurements with W/ D = 0.585, one measurement with W/D = 1.167, and one measurement with W/D = 0.292, in sample D (3.0 mm thick): (**a**) longitudinal and (**b**) transverse

and intermediate thickness samples for comparison to the measured residual stress.

We conclude that the thickness-dependent residual stress calculation procedure provides a meaningful improvement over the previously-published thick-workpiece residual stress calculation procedure. When comparing residual stresses calculated by both procedures to the expected residual stress, we find that the thick workpiece calculation procedure (when used, inappropriately, in a thin or intermediate workpiece) exaggerates the maxima and minima of the residual stress versus depth curve as compared to the thickness-dependent calculation procedure. This exaggeration increases as sample thickness decreases. Overall, measurement results from the thickness-dependent stress calculation procedure reflect the expectation of stress release by bending in samples removed from the thick plate, while the results from the thick-workpiece calculation do not.

We find that agreement between the measured residual stress and the expected residual stress (from FE) increases as sample thickness increases. For the two thickest samples (samples C and D), the measured residual stress closely matches the expected residual stress. For the two thinnest samples (A and B), there is noticeable disagreement between the measured and expected residual stress versus depth profiles; the disagreement includes near-surface stress (within 0.15 mm of the surface) and subsurface stress (depths from 0.3 to 0.6 mm). Further investigation of stress in the thinnest sample (sample A) suggested that the expected residual stress may have unaccounted-for systematic error, the error being most apparent in the thinnest sample.

We find that clamping has unexpected effects on measurements in the thinnest sample (sample A). Firm clamping of the thinnest sample produces measured residual stress that more closely matches the expected residual stress than the cantilever clamping strategy used for most measurements in the removed samples. However, because the firm clamping strategy breaks established good practice guidelines for hole-drilling, effects of sample clamping should be further studied.

A series of follow-on residual stress measurements using gages with different sizes confirms the usefulness of the thickness-dependent stress calculation procedure. When gage size was varied by a factor of 4, the measured strains changed considerably but the calculated residual stresses were largely invariant.

Acknowledgements The hole-drilling milling station was provided to UC Davis as an equipment loan from Hill Engineering, LLC (Rancho Cordova, CA USA), and was supported by Teresa Wong. The authors are grateful to Adrian DeWald and Brett Watanabe of Hill Engineering, LLC for providing the follow-on hole-drilling measurements with various hole sizes. This work was performed with funding from Los Alamos National Laboratory (LANL) through the Graduate Fellowships for STEM Diversity (GFSD) fellowship program. Any opinions, findings, and conclusions or recommendations expressed in this material are those of the authors and do not necessarily reflect the views of UC Davis, LANL, or GFSD.

Declarations

Competing Interests This study was performed by the authors with the support noted above. No authors report any competing interest that played a significant role in the work reported.

References

1. Schajer GS, Whitehead PS (2018) Hole drilling method for measuring residual stresses. Morgan & Claypool Publishers. https://doi.org/10.2200/S00818ED1V01Y201712SEM001
2. ASTM E837–20 (2020) Standard Test Method for Determining Residual Stresses by the Hole-Drilling Strain-Gage Method. Testing Standard, West Conshohocken, PA: ASTM International. https://doi.org/10.1520/E0837-20
3. Grant PV, Lord JD, Whitehead P (2006) NPL Good Practice Guide No. 53 – Issue 2. The Measurement of Residual Stresses by the Incremental Hole Drilling Technique. National Physical Laboratory, Hampton Road, Teddington, Middlesex, UK. Retrieved from https://eprintspublications.npl.co.uk/2517/1/mgpg53.pdf
4. Olson MD, DeWald AT, Hill MR (2021) (2020) Precision of hole-drilling residual stress depth profile measurements and an updated uncertainty estimator. Exp Mech 61:549–564. https://doi.org/10.1007/s11340-020-00679-1
5. Chighizola CR et al (2021) Intermethod comparison and evaluation of measured near surface residual stress in milled aluminum. Exp Mech. https://doi.org/10.1007/s11340-021-00734-5
6. Madariaga A, Perez I, Arrazola PJ, Sanchez R, Ruiz JJ, Rubio FJ (2018) Reduction of distortions in large aluminum parts by controlling machining-induced residual stresses. Int J Adv Manuf Technol 97:967–978. https://doi.org/10.1007/s00170-018-1965-2
7. Chigizola CR et al (2022) (2022) The effect of bulk residual stress on milling-induced residual stress and distortion. Exp Mech 62:1437–1459. https://doi.org/10.1007/s11340-022-00843-9
8. Lord JD, Penn D, Whitehead P (2008) The application of digital image correlation for measuring residual stress by incremental hole drilling. Appl Mech Mater 13:65–73. https://doi.org/10.4028/www.scientific.net/AMM.13-14.65
9. Peng Y, Zhao J, Chen LS, Dong J (2021) Residual stress measurement combining blind-hole drilling and digital image correlation approach. J Constr Steel Res 176:106346. https://doi.org/10.1016/j.jcsr.2020.106346
10. Schajer GS (2021) Compact calibration data for hole-drilling residual stress measurements in finite-thickness specimens. Exp Mech. https://doi.org/10.1007/s11340-020-00587-4
11. Luong H, Hill MR (2010) (2009) The effects of laser peening and shot peening on high cycle fatigue in 7050–T7451 aluminum alloy. Mater Sci Eng, A 527:699–707. https://doi.org/10.1016/j.msea.2009.08.045
12. Huang X, Sun J, Li J (2015) Finite element simulation and experimental investigation on the residual stress-related monolithic component deformation. Int J Adv Manuf Technol 77(5–8):1035–1041. https://doi.org/10.1007/s00170-014-6533-9
13. US Department of Defense (1998) MIL-HDBK-5H. Metallic materials and elements for aerospace vehicle structures. Washington, D.C.
14. Dessault Systemes Corporation (2014) ABAQUS/Standard User Manual. Version 6.14
15. Metal Improvement Company (2005) Shot peening applications, 9th Edition. Paramus, NJ. Retrieved from https://www.cwst.co.uk/wp-content/uploads/2015/08/MIC_Green_Book_9th_Edition.pdf
16. Gao YK (2011) (2011), Improvement of fatigue property in 7050–T7451 aluminum alloy by laser peening and shot peening. Mater Sci Eng, A 528:3823–3828. https://doi.org/10.1016/j.msea.2011.01.077
17. Carvalho ALM, Voorwald HJC (2009) The surface treatment influence on the fatigue crack propagation of Al 7050–T7451 alloy. Mater Sci Eng, A 209(505):31–40. https://doi.org/10.1016/j.msea.2008.10.053
18. Michaud April S (2007) Influence du grenaillage sur la vie en fatigue d'un alliage d'aluminium. Masters thesis, École Polytechnique de Montréal. Retreived from https://publications.polymtl.ca/7935/1/2007_MichaudApril.pdf